

**ARTICLE****A Suitable Active Control for Suppression the Vibrations of a Cantilever Beam**Y. A. Amer¹, A. T. EL-Sayed² and M. N. Abd EL-Salam^{3,*}¹Mathematics Department, Science Faculty, Zagazig University, Zagazig, Egypt²Basic Sciences Department, Modern Academy for Engineering and Technology, Cairo, Egypt³Basic Sciences Department, Higher Technological Institute, 10th of Ramadan City, Egypt

*Corresponding Author: M. N. Abd EL-Salam. Email: mansour.naserallah@yahoo.com

Received: 31 May 2020 Accepted: 24 December 2021

ABSTRACT

In our consideration, a comparison between four different types of controllers for suppression the vibrations of the cantilever beam excited by an external force is carried out. Those four types are the linear velocity feedback control, the cubic velocity feedback control, the non-linear saturation controller (NSC) and the positive position feedback (PPF) controller. The suitable type is the PPF controller for suppression the vibrations of the cantilever beam. The approximate solution obtained up to the first approximation by using the multiple scale method. The PPF controller effectiveness is studied on the system. We used frequency-response equations to investigate the stability of a cantilever beam. We notified that, there is a good agreement between the analytical solution and the numerical solution.

KEYWORDS

Cantilever beam; cubic velocity feedback control; linear velocity feedback control; non-linear saturation controller (NSC); positive position feedback (PPF) controller

1 Introduction

Many types of controllers are used for suppressing the vibrations of different non-linear dynamical systems such that, negative linear velocity feedback, negative cubic velocity feedback, non-linear saturation controllers (NSC), non-linear Integral Positive Position Feedback Controllers (NIPPF), the Integral resonant controllers (IRC) and time delay control. The technique of multiple time scales used to investigate the micro-beams non-linear vibrations for two different resonance cases (super-harmonic and harmonic resonances). From this investigation, there is a clear effect of the boundary conditions on the micro-beams vibrations [1]. Recently, the vibrations of many vibrating systems [2–7] has been studied. Because of the time delayed and active controls springiness [8–14] in controlling many vibrating system, many papers used time delay for suppressing the vibrations of non-linear systems. Abdelhafez et al. [15] investigated the effectiveness of time delays when the positive position controllers are used for suppressing the vibrations of a self-excited non-linear beam. They notified that, the time margin depends on the overall delays of the system $\tau_1 + \tau_2$. The authors in [16] investigated the influence of two different delays the first is displacement delay and the second is velocity delay in a cantilever beam. They used the method of multiple scales to determine all super-harmonic and sub-harmonic resonance cases.



Since the aim of most studies is to suppress the vibrations, one of the important types of control to vibrating systems is the PPF, which, described by a single degree of freedom system that, its frequency tuned to one of the structural frequencies. El-Ganaini et al. [17] presents the effectiveness of the PPF controller for decreasing the vibrations of nonlinear system at primary resonance and one-to-one internal resonance. They concluded that, PPF controller successful for systems that, has a small natural frequency. El-sayed et al. [18] achieved good results in decreasing the vibrations of vertical conveyor subject to external excitations by using PPF controllers such that, the vibrations in first mode reduced about 99.88% and the vibrations in the second mode reduced about 99.97% from its values without controllers. Ferrari et al. [19] offered an experimentally studying for the effectiveness of the PPF controllers on suspended the vibrations of sandwich plate. Niu et al. [20] realized the fractional-order positive position feedback (FOPPF) controller. They found that, the FOPPF controller gives better results comparing with PPF controller. Omid et al. [21,22] presented three kinds of control to suppress the vibrations of vibrating systems such that, the Integral resonant controllers (IRC), PPF controllers and the non-linear Integral Positive Position feedback (NIPPF). The eminent type of decreasing the vibrations is NIPPF type. PPF controller and multimode modified positive position feedback (MMPPF) controllers are used for decreasing the vibrations of a flexible beam and a collocated structure, respectively [23,24].

In this article, four types of active vibrations controllers the linear velocity feedback control, the cubic velocity feedback control, NSC and PPF controller used to suppression the vibrations of a cantilever beam containing the cubic and fifth nonlinearity terms excited by an external force. The positive position feedback controller (PPF) is the suitable active control type for decreasing the cantilever beam's vibrations. The approximate solution obtained applying the method of multiple scales up to first approximation. The stability of the cantilever beam investigated at the simultaneous resonance conditions (1:1 internal and primary). The behavior of the cantilever beam without and with PPF controller is simulated numerically. The influence of some chosen coefficient is illustrated numerically. The rapprochement between numeric and analytic solution is offered.

2 Mathematical Modelling

The equation of motion of a cantilever beam described by the following differential equation [15]:

$$\ddot{x} + \alpha_1 \dot{x} + \beta_1 \dot{x}^3 + \beta_2 \dot{x}^5 + \omega_1^2 x + \gamma_1 x^3 + \gamma_2 x^5 + \delta_1 (x \dot{x}^2 + x^2 \ddot{x}) + \delta_2 (x^3 \dot{x}^2 + x^4 \ddot{x}) = f \cos(\Omega t) \quad (1)$$

where, x is the displacement of the cantilever beam. The damping coefficient represented by α_1 . The nonlinearities terms coefficients are β_j , γ_j and δ_j ($j = 1, 2$). The excitation frequency and amplitude are Ω and f . For suppression the vibrations of the cantilever beam, we used four different types of controllers as the following.

The negative linear velocity feedback:

$$\begin{aligned} \ddot{x} + \varepsilon \hat{\alpha}_1 \dot{x} + \varepsilon \hat{\beta}_1 \dot{x}^3 + \varepsilon \hat{\beta}_2 \dot{x}^5 + \omega_1^2 x + \varepsilon \hat{\gamma}_1 x^3 + \varepsilon \hat{\gamma}_2 x^5 + \varepsilon \hat{\delta}_1 (x \dot{x}^2 + x^2 \ddot{x}) + \varepsilon \hat{\delta}_2 (x^3 \dot{x}^2 + x^4 \ddot{x}) \\ = \varepsilon \hat{f} \cos(\Omega t) - \varepsilon \hat{G}_1 \dot{x} \end{aligned} \quad (2)$$

The negative cubic velocity feedback:

$$\begin{aligned} \ddot{x} + \varepsilon \hat{\alpha}_1 \dot{x} + \varepsilon \hat{\beta}_1 \dot{x}^3 + \varepsilon \hat{\beta}_2 \dot{x}^5 + \omega_1^2 x + \varepsilon \hat{\gamma}_1 x^3 + \varepsilon \hat{\gamma}_2 x^5 + \varepsilon \hat{\delta}_1 (x \dot{x}^2 + x^2 \ddot{x}) + \varepsilon \hat{\delta}_2 (x^3 \dot{x}^2 + x^4 \ddot{x}) \\ = \varepsilon \hat{f} \cos(\Omega t) - \varepsilon \hat{G}_2 \dot{x}^3 \end{aligned} \quad (3)$$

The non-linear saturation controller:

$$\begin{aligned} \ddot{x} + \varepsilon\hat{\alpha}_1\dot{x} + \varepsilon\hat{\beta}_1\dot{x}^3 + \varepsilon\hat{\beta}_2\dot{x}^5 + \omega_1^2x + \varepsilon\hat{\gamma}_1x^3 + \varepsilon\hat{\gamma}_2x^5 + \varepsilon\hat{\delta}_1(x\dot{x}^2 + x^2\ddot{x}) + \varepsilon\hat{\delta}_2(x^3\dot{x}^2 + x^4\ddot{x}) \\ = \varepsilon\hat{f}\cos(\Omega t) + \varepsilon\hat{\eta}_1y^2 \end{aligned} \quad (4a)$$

$$\ddot{y} + \varepsilon\hat{\alpha}_2\dot{y} + \omega_2^2y = \varepsilon\hat{\eta}_2xy \quad (4b)$$

The positive position feedback controller:

$$\begin{aligned} \ddot{x} + \varepsilon\hat{\alpha}_1\dot{x} + \varepsilon\hat{\beta}_1\dot{x}^3 + \varepsilon\hat{\beta}_2\dot{x}^5 + \omega_1^2x + \varepsilon\hat{\gamma}_1x^3 + \varepsilon\hat{\gamma}_2x^5 + \varepsilon\hat{\delta}_1(x\dot{x}^2 + x^2\ddot{x}) + \varepsilon\hat{\delta}_2(x^3\dot{x}^2 + x^4\ddot{x}) \\ = \varepsilon\hat{f}\cos(\Omega t) + \varepsilon\hat{\lambda}_1y \end{aligned} \quad (5a)$$

$$\ddot{y} + \varepsilon\hat{\alpha}_2\dot{y} + \omega_2^2y = \varepsilon\hat{\lambda}_2x \quad (5b)$$

where, ω_1 and ω_2 are the natural frequencies of the cantilever beam and the PPF controller. The control and feedback signals are $\hat{\lambda}_1$, $\hat{\eta}_1$, and $\hat{\lambda}_2$, $\hat{\eta}_2$. The feedback gains are \hat{G}_1 and \hat{G}_2 . To summarize the comparison between the four types of control, we explain the flowchart diagram as in Fig. 1.

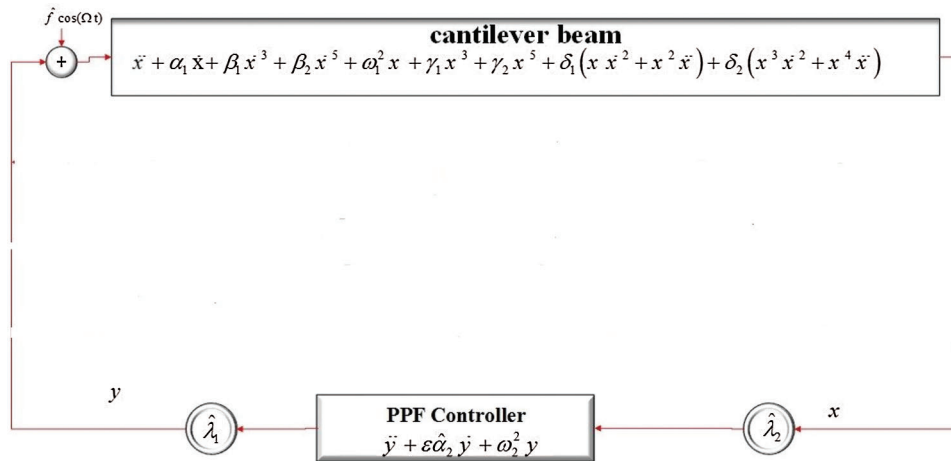


Figure 1: The flowchart diagram of the main system with PPF controller

2.1 Time History with Numerical Simulation

Numerically, the cantilever beam's differential Eq. (1) was studied using Runge-Kutta 4th order method at the worst resonance case (One-to-one internal and primary resonance) at the following values of parameters:

$$\omega_1 = 1.4, \beta_1 = 0.3331, \beta_2 = 0.1299, \gamma_1 = 0.3338, \gamma_2 = 0.1319, \delta_1 = 3.2746, \delta_2 = 2.2, \alpha_1 = 0.005, f = 0.01$$

At this study, we compare between four different types of controllers for suppressing the vibration of a cantilever beam. Fig. 2 presents the uncontrolled cantilever beam before using any type of controllers at the primary resonance case. In Fig. 3, we used two types of controllers to decrease the vibration of the system. The first type, is a negative cubic velocity feedback control which decreasing the vibration of the system to reach 0.13, so, the effectiveness of the control (E_a = amplitude of uncontrolled system/amplitude of controlled system) equal one as shown in Fig. 3a. The second type, is a negative linear velocity feedback

control which decreasing the vibration of the system to reach 0.007, so, the effectiveness of the control $E_a = 21$ as shown in Fig. 3b. Fig. 4 illustrates the effectiveness of the non-linear saturation controller (NSC) on the cantilever beam. From this figure, we concluded that, the NSC controller minimized the vibration to reach 0.07 which means that $E_a = 2$. The positive position feedback controller (PPF) is the best type of controllers for suppressing the vibrations of the cantilever beam where it reduced the vibrations to 0.0006 and $E_a = 250$ as shown in Fig. 5. The solid lines elucidated the numerical solution of the main system before and after using the PPF controller while, dash lines elucidated the amplitude adjustments a_1 and a_2 for the generalized coordinates x and y . Finally, there is a good agreement between the numerical and analytical solutions of the main system and the PPF controller as presented in Figs. 2 and 5.

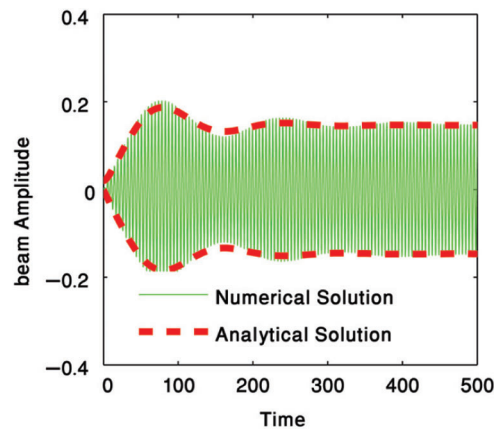


Figure 2: Uncontrolled system at primary resonance case

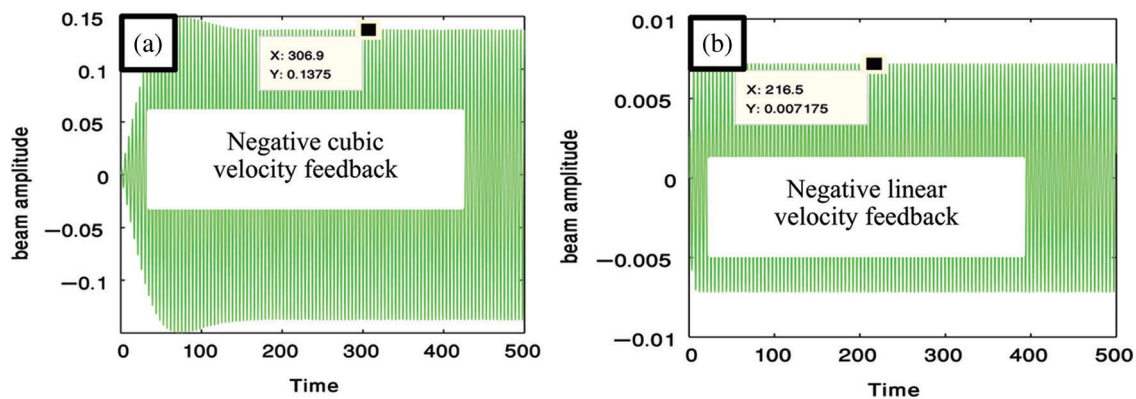


Figure 3: Negative cubic and linear velocity feedback for reducing the amplitude of the cantilever beam

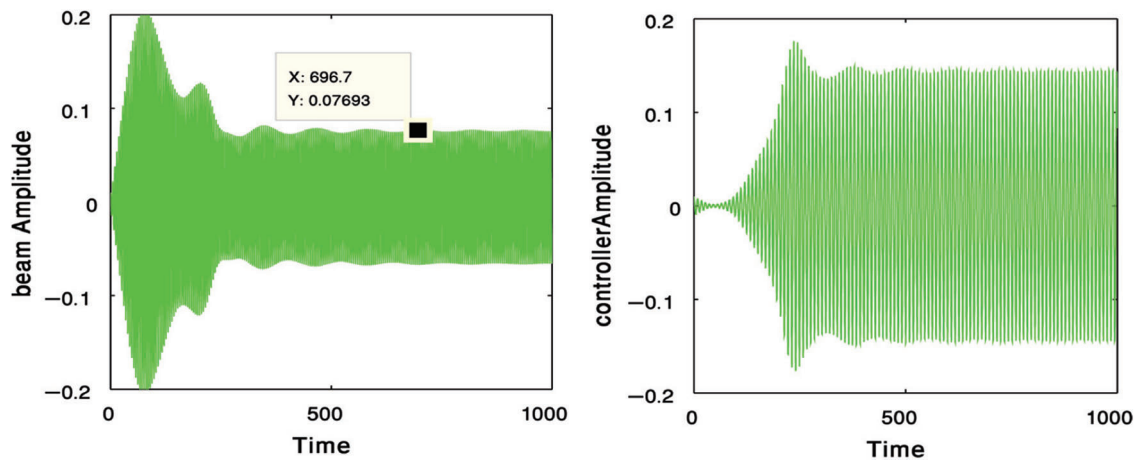


Figure 4: NSC controller for reducing the amplitude of the main system

2.2 Perturbation Analysis

According to the results that we obtained from Fig. 5, Which shows that the most appropriate controller is the PPF controller so we will study the main system after activating the PPF control. To get the approximate solution up to the first approximation, we applied the method of multiple scales [25,26] as the following:

$$\left. \begin{aligned} x(t; \varepsilon) &= x_0(T_0, T_1) + \varepsilon x_1(T_0, T_1) + O(\varepsilon^2) \\ y(t; \varepsilon) &= y_0(T_0, T_1) + \varepsilon y_1(T_0, T_1) + O(\varepsilon^2) \end{aligned} \right\} \quad (6)$$

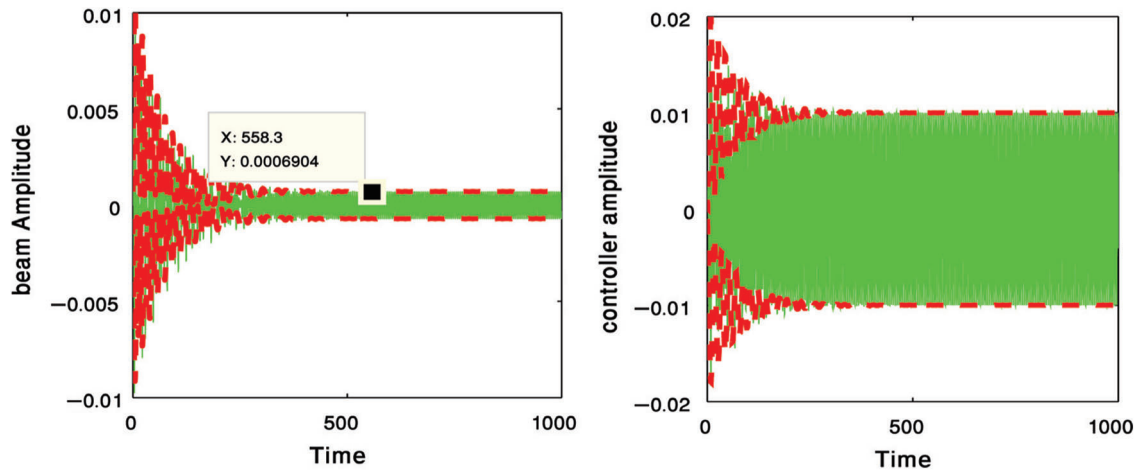


Figure 5: PPF controller for reducing the amplitude of the main system

where, the fast scale is T_0 and the slow scale is $T_1 = \varepsilon t$. The derivatives using the multiple scales method take the forms:

$$\left. \begin{aligned} \frac{d}{dt} &= D_0 + \varepsilon D_1 + \dots \\ \frac{d^2}{dt^2} &= D_0^2 + 2\varepsilon D_0 D_1 + \dots \end{aligned} \right\} D_j = \frac{\partial}{\partial T_j} \quad (j = 0, 1) \quad (7)$$

Inserting Eqs. (4) and (5) in Eqs. (2) and (3) such that:

$$[D_0^2 + \omega_1^2]x_0 + \varepsilon[D_0^2 + \omega_1^2]x_1 = \varepsilon \left\{ \begin{aligned} &\hat{f} \cos(\Omega t) + \hat{\lambda}_1 y_0 - \hat{\gamma}_1 x_0^3 - \hat{\gamma}_2 x_0^5 \\ &- 2D_0 D_1 x_0 - \hat{\alpha}_1 D_0 x_0 - \hat{\beta}_1 (D_0 x_0)^3 \\ &-\hat{\beta}_2 (D_0 x_0)^5 - \hat{\delta}_1 (x_0 (D_0 x_0)^2 + x_0^2 D_0^2 x_0) \\ &-\hat{\delta}_2 (x_0^3 (D_0 x_0)^2 + x_0^4 D_0^2 x_0) \end{aligned} \right\} + O(\varepsilon^2) \quad (8)$$

$$[D_0^2 + \omega_2^2]y_0 + \varepsilon[D_0^2 + \omega_2^2]y_1 = \varepsilon [\hat{\lambda}_2 x_0 - 2D_0 D_1 y_0 - \hat{\alpha}_2 D_0 y_0] + O(\varepsilon^2) \quad (9)$$

Equating the coefficients of the same power of ε :

$O(\varepsilon^0)$:

$$[D_0^2 + \omega_1^2]x_0 = 0 \quad (10)$$

$$[D_0^2 + \omega_2^2]y_0 = 0 \quad (11)$$

$O(\varepsilon)$:

$$[D_0^2 + \omega_1^2]x_1 = \left\{ \begin{aligned} &\hat{f} \cos(\Omega t) + \hat{\lambda}_1 y_0 - \hat{\gamma}_1 x_0^3 - \hat{\gamma}_2 x_0^5 - 2D_0 D_1 x_0 - \hat{\alpha}_1 D_0 x_0 - \hat{\beta}_1 (D_0 x_0)^3 \\ &-\hat{\beta}_2 (D_0 x_0)^5 - \hat{\delta}_1 (x_0 (D_0 x_0)^2 + x_0^2 D_0^2 x_0) - \hat{\delta}_2 (x_0^3 (D_0 x_0)^2 + x_0^4 D_0^2 x_0) \end{aligned} \right\} \quad (12)$$

$$[D_0^2 + \omega_2^2]y_1 = [\hat{\lambda}_2 x_0 - 2D_0 D_1 y_0 - \hat{\alpha}_2 D_0 y_0] \quad (13)$$

Solving the homogenous differential Eqs. (10) and (11) to get the following:

$$x_0(T_0, T_1) = A(T_1) e^{i\omega_1 T_0} + \bar{A}(T_1) e^{-i\omega_1 T_0} \quad (14)$$

$$y_0(T_0, T_1) = B(T_1) e^{i\omega_2 T_0} + \bar{B}(T_1) e^{-i\omega_2 T_0} \quad (15)$$

Denote that A and B , are complex functions in T_1 . For computation the right hand sides of Eqs. (12) and (13), we will replace x_0 and y_0 by its values in Eqs. (14) and (15) so that:

$$[D_0^2 + \omega_1^2]x_1 = \left\{ \begin{aligned} &\left[\begin{aligned} &-2i\omega_1 D_1 A - i\hat{\alpha}_1 \omega_1 A - 3i\hat{\beta}_1 \omega_1^3 A^2 \bar{A} - 10i\hat{\beta}_2 \omega_1^5 A^3 \bar{A}^2 - 3\hat{\gamma}_1 A^2 \bar{A} \end{aligned} \right] e^{i\omega_1 T_0} \\ &+ \left[\begin{aligned} &+2\hat{\delta}_1 \omega_1^2 A^2 \bar{A} - 10\hat{\gamma}_2 A^3 \bar{A}^2 + 8\hat{\delta}_2 \omega_1^2 A^3 \bar{A}^2 \\ &+ i\hat{\beta}_1 \omega_1^3 A^3 + 5i\hat{\beta}_2 \omega_1^5 A^4 \bar{A} - \hat{\gamma}_1 A^3 - 5\hat{\gamma}_2 A^4 \bar{A} + 2\hat{\delta}_1 \omega_1^2 A^3 \end{aligned} \right] e^{3i\omega_1 T_0} \\ &+ \left[\begin{aligned} &+6\hat{\delta}_2 \omega_1^2 A^4 \bar{A} \\ &+ [-i\hat{\beta}_2 \omega_1^5 A^5 - \hat{\gamma}_2 A^5 + 2\hat{\delta}_2 \omega_1^2 A^5] e^{5i\omega_1 T_0} + [\hat{\lambda}_1 B] e^{i\omega_2 T_0} + \left[\frac{\hat{f}}{2} \right] e^{i\Omega T_0} \end{aligned} \right] \end{aligned} \right\} + CC \quad (16)$$

$$[D_0^2 + \omega_2^2]y_1 = [-2i\omega_2 D_1 B - i\hat{\alpha}_2 \omega_2 B] e^{i\omega_2 T_0} + [\hat{\lambda}_2 A] e^{i\omega_1 T_0} + CC \quad (17)$$

The complex conjugate parts collected in the term CC. For getting the particular solutions of Eqs. (16) and (17), we will remove the secular terms such that:

$$x_1(T_0, T_1) = H_1(T_1) e^{3i\omega_1 T_0} + H_2(T_1) e^{5i\omega_1 T_0} + H_3(T_1) e^{i\omega_2 T_0} + H_4(T_1) e^{i\Omega T_0} + CC \quad (18)$$

$$y_1(T_0, T_1) = H_5(T_1) e^{i\omega_1 T_0} + CC \quad (19)$$

where H_j ($j = 1, \dots, 5$) offering complex functions in T_1 which defined in the appendix. From the first approximation, we concluded the following resonance cases:

- i) Primary resonance: $\Omega \cong \omega_1$
- ii) Internal resonance: $\omega_1 \cong \omega_2$
- iii) Simultaneous resonance: One-to-one internal and primary resonance.

3 Periodic Solutions

In this section, the selected one is simultaneous resonance ($\Omega \cong \omega_1, \omega_1 \cong \omega_2$) is used to discuss the solvability conditions, we will introduce two detuning parameters (σ_1, σ_2) so that:

$$\left. \begin{aligned} \Omega &= \omega_1 + \varepsilon \hat{\sigma}_1 = \omega_1 + \sigma_1 \\ \omega_2 &= \omega_1 + \varepsilon \hat{\sigma}_2 = \omega_1 + \sigma_2 \end{aligned} \right\} \quad (20)$$

Including Eq. (20) into Eqs. (16) and (17) for compiling the solvability conditions as:

$$\begin{aligned} -2i\omega_1 D_1 A - i\hat{\alpha}_1 \omega_1 A - 3i\hat{\beta}_1 \omega_1^3 A^2 \bar{A} - 10i\hat{\beta}_2 \omega_1^5 A^3 \bar{A}^2 + (2\hat{\delta}_1 \omega_1^2 - 3\hat{\gamma}_1) A^2 \bar{A} + (8\hat{\delta}_2 \omega_1^2 - 10\hat{\gamma}_2) A^3 \bar{A}^2 \\ + \frac{\hat{f}}{2} e^{i\hat{\sigma}_1 T_1} + \hat{\lambda}_1 B e^{i\hat{\sigma}_2 T_1} = 0 \end{aligned} \quad (21)$$

$$-2i\omega_2 D_1 B - i\hat{\alpha}_2 \omega_2 B + \hat{\lambda}_2 A e^{-i\hat{\sigma}_2 T_1} = 0 \quad (22)$$

Exchanging A and B by the polar form as:

$$\left. \begin{aligned} A(T_1) &= a_1(T_1) e^{i\theta_1(T_1)} \\ B(T_1) &= a_2(T_1) e^{i\theta_2(T_1)} \\ D_1 A(T_1) &= (a'_1(T_1) + ia_1 \theta'_1(T_1)) e^{i\theta_1(T_1)} \\ D_1 B(T_1) &= (a'_2(T_1) + ia_2 \theta'_2(T_1)) e^{i\theta_2(T_1)} \end{aligned} \right\}; \quad (\cdot)' = \frac{d}{dT_1} \quad (23)$$

where a_j and θ_j ($j = 1, 2$) are the motion's steady state phases and amplitudes. Subjoining Eq. (23) into Eqs. (21) and (22). For any two equal complex numbers, the real and imaginary parts are equal so that:

$$a'_1 = \left[-\frac{\hat{\alpha}_1}{2} \right] a_1 - \left[\frac{3\hat{\beta}_1 \omega_1^2}{8} \right] a_1^3 - \left[\frac{5\hat{\beta}_2 \omega_1^4}{16} \right] a_1^5 + \left[\frac{\hat{f}}{2\omega_1} \right] \sin \phi_1 + \left[\frac{\hat{\lambda}_1}{2\omega_1} \right] a_2 \sin \phi_2 \quad (24)$$

$$a_1 \theta'_1 = \left[\frac{3\hat{\gamma}_1}{8\omega_1} - \frac{\hat{\delta}_1 \omega_1}{4} \right] a_1^3 + \left[\frac{5\hat{\gamma}_2}{16\omega_1} - \frac{\hat{\delta}_2 \omega_1}{4} \right] a_1^5 - \left[\frac{\hat{f}}{2\omega_1} \right] \cos \phi_1 - \left[\frac{\hat{\lambda}_1}{2\omega_1} \right] a_2 \cos \phi_2 \quad (25)$$

$$a'_2 = \left[-\frac{\hat{\alpha}_2}{2}\right] a_2 - \left[\frac{\hat{\lambda}_2}{2\omega_2}\right] a_1 \sin \phi_2 \quad (26)$$

$$a_2 \theta'_2 = -\left[\frac{\hat{\lambda}_2}{2\omega_2}\right] a_1 \cos \phi_2 \quad (27)$$

where, $\phi_1 = \hat{\sigma}_1 T_1 - \theta_1$ and $\phi_2 = \hat{\sigma}_2 T_1 + \theta_2 - \theta_1$. Back to the main system parameters, we have the following equations:

$$\dot{a}_1 = \left[-\frac{\alpha_1}{2}\right] a_1 - \left[\frac{3\beta_1\omega_1^2}{8}\right] a_1^3 - \left[\frac{5\beta_2\omega_1^4}{16}\right] a_1^5 + \left[\frac{f}{2\omega_1}\right] \sin \phi_1 + \left[\frac{\lambda_1}{2\omega_1}\right] a_2 \sin \phi_2 \quad (28)$$

$$a_1 \dot{\theta}_1 = \left[\frac{3\gamma_1}{8\omega_1} - \frac{\delta_1\omega_1}{4}\right] a_1^3 + \left[\frac{5\gamma_2}{16\omega_1} - \frac{\delta_2\omega_1}{4}\right] a_1^5 - \left[\frac{f}{2\omega_1}\right] \cos \phi_1 - \left[\frac{\lambda_1}{2\omega_1}\right] a_2 \cos \phi_2 \quad (29)$$

$$\dot{a}_2 = \left[-\frac{\alpha_2}{2}\right] a_2 - \left[\frac{\lambda_2}{2\omega_2}\right] a_1 \sin \phi_2 \quad (30)$$

$$a_2 \dot{\theta}_2 = -\left[\frac{\lambda_2}{2\omega_2}\right] a_1 \cos \phi_2 \quad (31)$$

where, $a'_1 = \frac{\dot{a}_1}{\varepsilon}$, $a'_2 = \frac{\dot{a}_2}{\varepsilon}$, $\theta'_1 = \frac{\dot{\theta}_1}{\varepsilon}$, $\theta'_2 = \frac{\dot{\theta}_2}{\varepsilon}$ and $(\dot{}) = \frac{d}{dt}$.

3.1 Fixed Point Solution

For steady-state solution, we maybe find the fixed point of the Eqs. (28)–(31) by putting $\dot{a}_1 = \dot{a}_2 = 0$ and $\dot{\phi}_j = 0$ ($j = 1, 2$), so:

$$0 = \left[-\frac{\alpha_1}{2}\right] a_1 - \left[\frac{3\beta_1\omega_1^2}{8}\right] a_1^3 - \left[\frac{5\beta_2\omega_1^4}{16}\right] a_1^5 + \left[\frac{f}{2\omega_1}\right] \sin \phi_1 + \left[\frac{\lambda_1}{2\omega_1}\right] a_2 \sin \phi_2 \quad (32)$$

$$a\sigma_1 = \left[\frac{3\gamma_1}{8\omega_1} - \frac{\delta_1\omega_1}{4}\right] a_1^3 + \left[\frac{5\gamma_2}{16\omega_1} - \frac{\delta_2\omega_1}{4}\right] a_1^5 - \left[\frac{f}{2\omega_1}\right] \cos \phi_1 - \left[\frac{\lambda_1}{2\omega_1}\right] a_2 \cos \phi_2 \quad (33)$$

$$0 = \left[-\frac{\alpha_2}{2}\right] a_2 - \left[\frac{\lambda_2}{2\omega_2}\right] a_1 \sin \phi_2 \quad (34)$$

$$a_2(\sigma_1 - \sigma_2) = -\left[\frac{\lambda_2}{2\omega_2}\right] a_1 \cos \phi_2 \quad (35)$$

From the preceding system, the trigonometric functions can be written as:

$$\sin \phi_1 = \left[\frac{2\omega_1}{f}\right] \left\{ \left[\frac{\alpha_1}{2}\right] a_1 + \left[\frac{3\beta_1\omega_1^2}{8}\right] a_1^3 + \left[\frac{5\beta_2\omega_1^4}{16}\right] a_1^5 + \left[\frac{\lambda_1\omega_2\alpha_2}{2\omega_1\lambda_2}\right] \frac{a_2^2}{a_1} \right\} \quad (36)$$

$$\cos \phi_1 = \left[\frac{2\omega_1}{f} \right] \left\{ \left[\frac{3\gamma_1}{8\omega_1} - \frac{\delta_1\omega_1}{4} \right] a_1^3 + \left[\frac{5\gamma_2}{16\omega_1} - \frac{\delta_2\omega_1}{4} \right] a_1^5 + \left[\frac{\lambda_1(\sigma_1 - \sigma_2)\omega_2}{\lambda_2\omega_1} \right] \frac{a_2^2}{a_1} - \sigma_1 a_1 \right\} \quad (37)$$

$$\sin \phi_2 = - \left[\frac{\omega_2\alpha_2}{\lambda_2} \right] \frac{a_2}{a_1} \quad (38)$$

$$\cos \phi_2 = - \left[\frac{2(\sigma_1 - \sigma_2)\omega_2}{\lambda_2} \right] \frac{a_2}{a_1} \quad (39)$$

Squaring then adding both sides of Eqs. (36) and (37) and Eqs. (38) and (39) to obtain the following two equations:

$$\left\{ \left[\frac{3\gamma_1}{8\omega_1} - \frac{\delta_1\omega_1}{4} \right] a_1^3 + \left[\frac{5\gamma_2}{16\omega_1} - \frac{\delta_2\omega_1}{4} \right] a_1^5 + \left[\frac{\lambda_1(\sigma_1 - \sigma_2)\omega_2}{\lambda_2\omega_1} \right] \frac{a_2^2}{a_1} - \sigma_1 a_1 \right\}^2 + \left\{ \left[\frac{\alpha_1}{2} \right] a_1 + \left[\frac{3\beta_1\omega_1^2}{8} \right] a_1^3 + \left[\frac{5\beta_2\omega_1^4}{16} \right] a_1^5 + \left[\frac{\lambda_1\omega_2\alpha_2}{2\omega_1\lambda_2} \right] \frac{a_2^2}{a_1} \right\}^2 = \left\{ \frac{f}{2\omega_1} \right\}^2 \quad (40)$$

$$\omega_2^2 [4\sigma_1^2 + 8\sigma_1\sigma_2 + 4\sigma_2^2 + \alpha_2^2] a_2^2 = [\lambda_2 a_1]^2 \quad (41)$$

3.2 Equilibrium Solution of a Fixed Point

While in movement to evolve the steady state solution's stability, start with the following procedures:

$$\left. \begin{aligned} a_1 &= a_{10} + a_{11} \\ a_2 &= a_{20} + a_{21} \\ \phi_1 &= \phi_{10} + \phi_{11} \\ \phi_2 &= \phi_{20} + \phi_{21} \end{aligned} \right\} \quad (42)$$

where, a_{10} , a_{20} , ϕ_{10} and ϕ_{20} are the solutions of Eqs. (32)–(35). The perturbations a_{11} , a_{21} , ϕ_{11} and ϕ_{21} are very small comparing with a_{10} , a_{20} , ϕ_{10} and ϕ_{20} so, after substituting from Eq. (42) into Eqs. (28)–(31) we keep only the linear terms of a_{11} , a_{21} , ϕ_{11} and ϕ_{21} . From this procedure, we get the following system:

$$\dot{a}_{11} = r_{11}a_{11} + r_{12}\phi_{11} + r_{13}a_{21} + r_{14}\phi_{21} \quad (43)$$

$$\dot{\phi}_{11} = r_{21}a_{11} + r_{22}\phi_{11} + r_{23}a_{21} + r_{24}\phi_{21} \quad (44)$$

$$\dot{a}_{21} = r_{31}a_{11} + r_{32}\phi_{11} + r_{33}a_{21} + r_{34}\phi_{21} \quad (45)$$

$$\dot{\phi}_{21} = r_{41}a_{11} + r_{42}\phi_{11} + r_{43}a_{21} + r_{44}\phi_{21} \quad (46)$$

In the appendix, we defined the coefficients r_{ij} ($i = 1 \dots 4$), ($j = 1 \dots 4$). The matrix form of the previous system can be written as:

$$\begin{bmatrix} \dot{a}_{11} & \dot{\phi}_{11} & \dot{a}_{21} & \dot{\phi}_{21} \end{bmatrix}^T = [D] \begin{bmatrix} a_{11} & \phi_{11} & a_{21} & \phi_{21} \end{bmatrix}^T \quad (47)$$

where $[D]$ is the Jacobian of the previous Eqs. (43)–(46). The Eigen-values of $[D]$ determined from extract the following determinant:

$$\begin{vmatrix} \lambda - r_{11} & r_{12} & r_{13} & r_{14} \\ r_{21} & \lambda - r_{22} & r_{23} & r_{24} \\ r_{31} & r_{32} & \lambda - r_{33} & r_{34} \\ r_{41} & r_{42} & r_{43} & \lambda - r_{44} \end{vmatrix} = 0 \quad (48)$$

which, are the roots of the following polynomial:

$$\lambda^4 + \Gamma_1\lambda^3 + \Gamma_2\lambda^2 + \Gamma_3\lambda + \Gamma_4 = 0 \quad (49)$$

where Γ_i ; ($i = 1, \dots, 4$) are the coefficients of Eq. (49) that, defined in the appendix. For the above system's solution to be stable, the Routh-Hurwitz criterion must be satisfied such that:

$$\Gamma_1 > 0, \Gamma_1\Gamma_2 - \Gamma_3 > 0, \Gamma_3(\Gamma_1\Gamma_2 - \Gamma_3) - \Gamma_1^2\Gamma_4 > 0, \Gamma_4 > 0 \quad (50)$$

4 Numerical Investigation

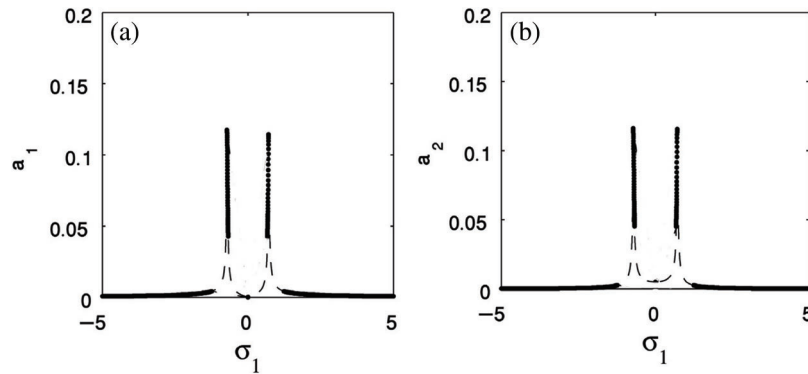


Figure 6: The response curves (a) The cantilever beam (b) The PPF controller

Eqs. (40) and (41) solved numerically to obtain the graphical solution for the amplitudes of both cantilever beam and the PPF controller via the detuning parameter (σ_1) which, represented by two peaks. Fig. 6 presents the frequency response curves of the cantilever beam and the PPF controller where, the stable solution represented by the solid line and the dash one using for the unstable solution. From this figure, we concluded that the minimum value of the cantilever beam amplitude occurs at $\sigma_1 = 0$ which means that, the PPF controller is capable of suppress the vibrations of the cantilever beam at the primary resonance case. For increasing values of a harmonic excitation force, the amplitudes of both the main system and the PPF controller increase, the jump phenomena occurs and the minimum value of the cantilever beam amplitude occurs at $\sigma_1 = 0$ as illustrates in Figs. 7a and 7b.

For small values of natural frequency for $\sigma_2 = 0$, i.e., ($\omega_1 = \omega_2$), the cantilever peak amplitude and the PPF controller peak amplitude increases and the bandwidth of the vibration reduction increases so, in the case of small natural frequency the PPF controller is very acceptable as shown in Fig. 8. The bandwidth of the vibration reduction of the main system increases by increasing the values of the control signal λ_1 and the feedback signal λ_2 as represented in Figs. 9a and 10a. Fig. 9b shows that the PPF controller amplitude is monotonic decreasing function of the control signal λ_1 . Fig. 10b shows that the PPF controller amplitude is monotonic increasing function of the feedback signal λ_2 . For three different values of the internal detuning parameter σ_2 , Fig. 11 shows the frequency response curves of both the cantilever beam and PPF

controller. From this figure, the minimum of the steady state amplitudes of both the cantilever beam and PPF controller happens when $\sigma_1 = \sigma_2$. From Fig. 12, there is a good agreement between the frequency response curves (FRC) which given by the solid line and the numerical solution of Eq. (1) using (RK-4) that marked by green circles.

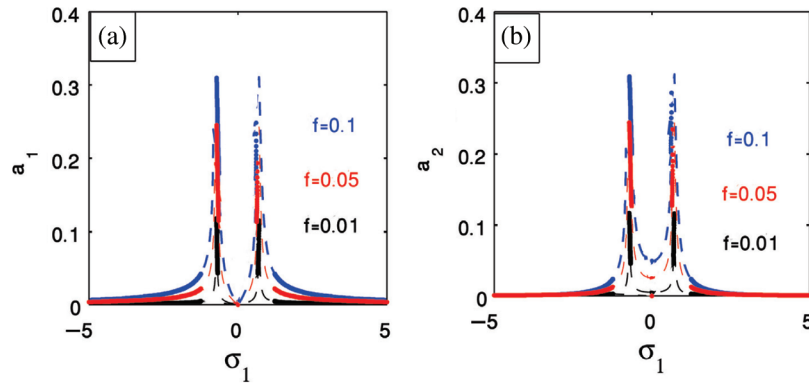


Figure 7: External force efficacy on (a) The cantilever beam (b) The PPF controller

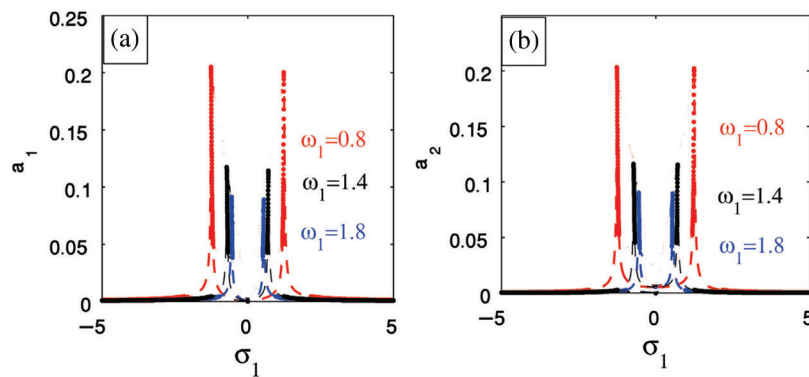


Figure 8: Natural frequency efficacy on (a) The cantilever beam (b) The PPF controller

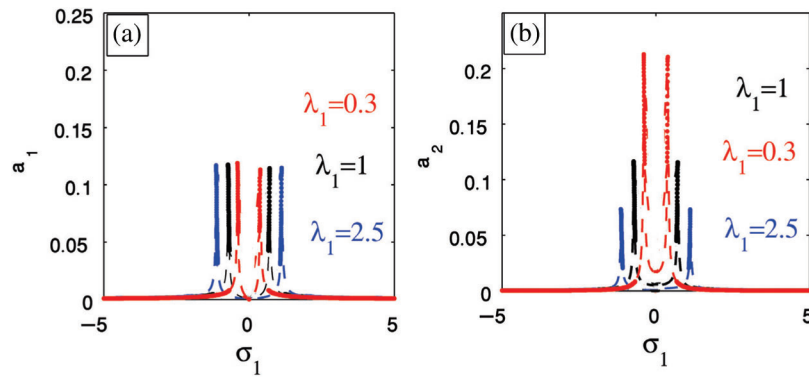


Figure 9: Control signal λ_1 efficacy on (a) The cantilever beam (b) The PPF controller

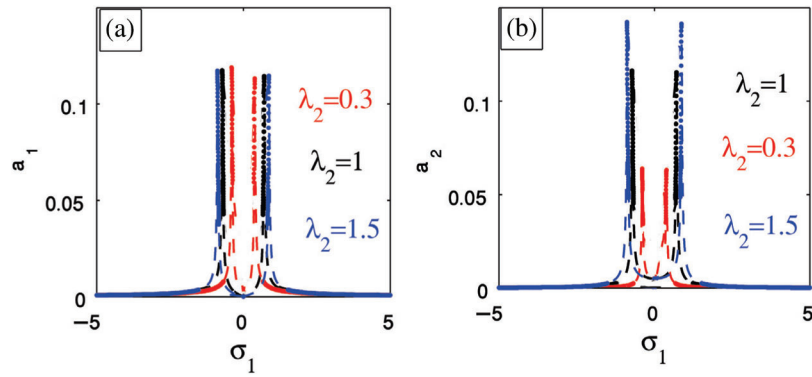


Figure 10: Feedback signal λ_2 efficacy on (a) The cantilever beam (b) The PPF controller

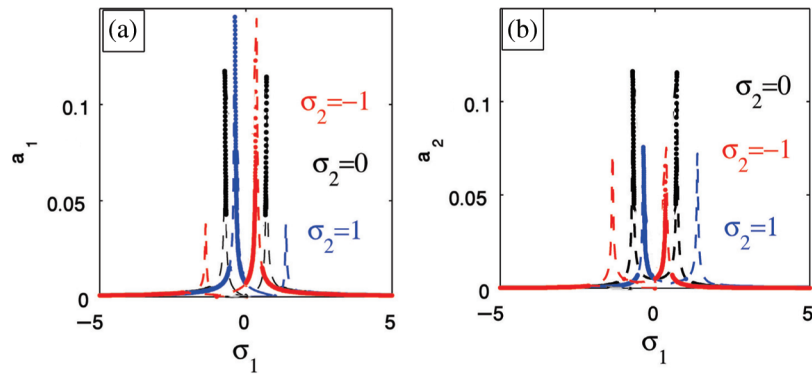


Figure 11: Detuning parameter σ_2 efficacy on (a) The cantilever beam (b) The PPF controller

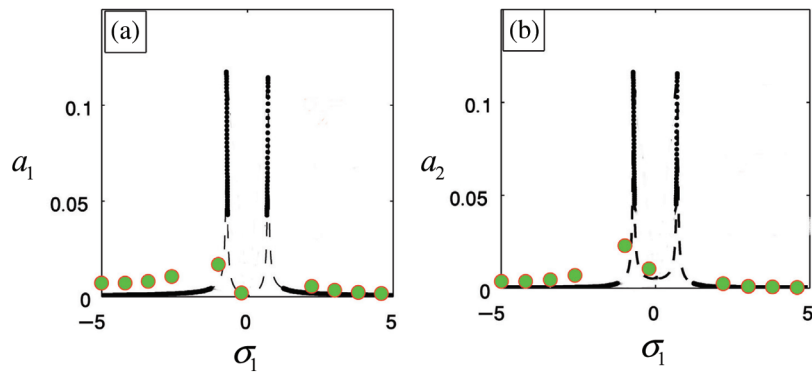


Figure 12: Comparison between the FRC solution and RK-4 solution

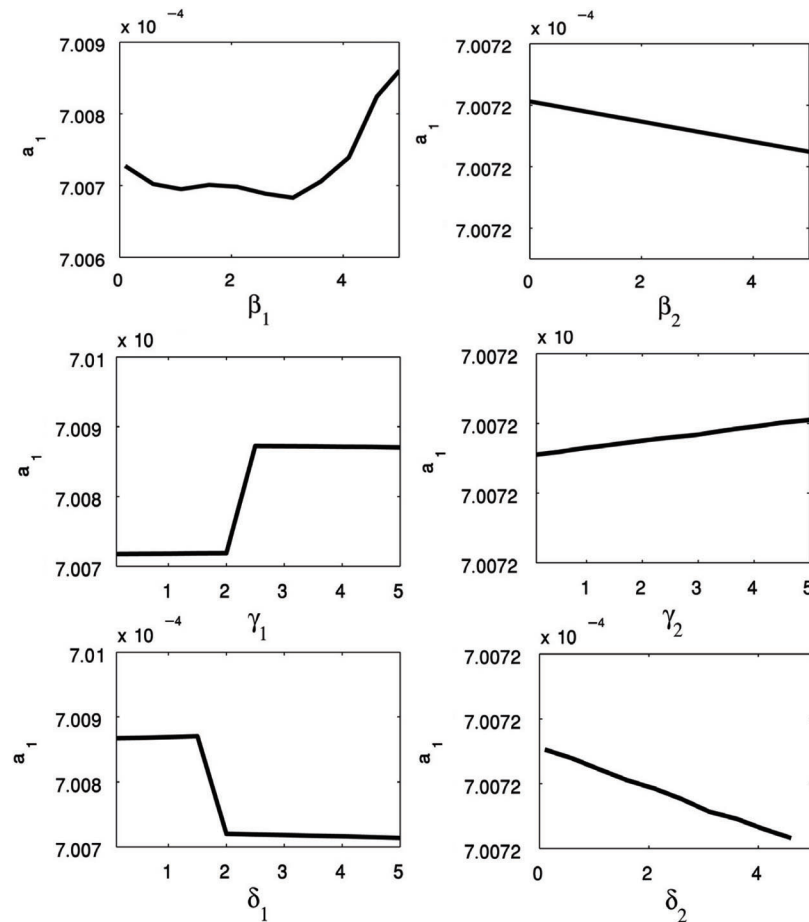


Figure 13: The influence of the nonlinear parameters on the main system amplitude

4.1 Influence of the Nonlinear Parameters

In the presence of the PPF controller, we studied the effectiveness of increases of all nonlinear parameters on the main system. The amplitude of the main system change either in decreasing or in increasing but this effect is very small so it do not appear clearly. For the nonlinear parameters β_1 , γ_1 and δ_1 , the range of the amplitude of the main system from 0.00070069 to 0.00070087 as observed on Figs. 13a, 13c and 13e. For the nonlinear parameters β_2 , γ_2 and δ_2 , the range of the amplitude of the main system from 0.00070071734 to 0.00070071736 as observed on Figs. 13b, 13d and 13f.

5 Conclusion

In this paper, we used four different types of active controllers for suppression the vibrations of the cantilever beam excited by an external force. Those four types are the linear velocity feedback control, the cubic velocity feedback control, the non-linear saturation controller (NSC) and the positive position feedback (PPF) controller. The best active control type for suppression the vibrations of the cantilever beam at the primary resonance case is the positive position feedback controller PPF as the following reasons:

- Its effectiveness E_a equal 250 which more than the effectiveness of any type of controllers used to control the vibrating cantilever beam in this study.
- It is a suitable for small natural frequencies as the bandwidth of the vibration reduction increases.

Farther more, the steady state amplitude is monotonic increasing function on the external excitation force. The bandwidth of the vibration reduction increases for increasing values of the control signal λ_1 and the feedback signal λ_2 . Finally, there is a good agreement between the frequency response curves (FRC) and the numerical solution using (RK-4). The nonlinear parameters have a very small effect either in decreasing or in increasing the main system amplitude.

Funding Statement: The authors received no specific funding for this study.

Conflicts of Interest: The authors declare that they have no conflicts of interest to report regarding the present study.

References

1. Onur Ekici, H., Boyaci, H. (2007). Effects of non-ideal boundary conditions on vibrations of microbeams. *Journal of Vibration and Control*, 13, 1369–1378. DOI 10.1177/1077546307077453.
2. Kuang, J. H., Chen, C. J. (2004). Dynamic characteristics of shaped micro-actuators solved using the differential quadrature method. *Journal of Micromechanics and Microengineering*, 14, 647–655. DOI 10.1088/0960-1317/14/4/028.
3. Abdel-Rahman, E. M., Younis, M. I., Nayfeh, A. H. (2002). Characterization of the mechanical behavior of an electrically actuated microbeam. *Journal of Micromechanics and Microengineering*, 12(6), 759–766. DOI 10.1088/0960-1317/12/6/306.
4. Younis, M. I., Nayfeh, A. H. (2003). A study of the nonlinear response of a resonant microbeam to an electric actuation. *Nonlinear Dynamics*, 31(1), 91–117. DOI 10.1023/A:1022103118330.
5. Amer, Y. A., EL-Sayed, A. T., EL-Salam, M. A. (2018). Non-linear saturation controller to reduce the vibrations of vertical conveyor subjected to external excitation. *Asian Research Journal of Mathematics*, 11(2), 1–26. DOI 10.9734/ARJOM/2018/44590.
6. Eftekhari, M., Ziaei-Rad, S., Mahzoon, M. (2013). Vibration suppression of a symmetrically cantilever composite beam using internal resonance under chordwise base excitation. *International Journal of Non-Linear Mechanics*, 48, 86–100. DOI 10.1016/j.ijnonlinmec.2012.06.011.
7. Nayfeh, A. H., Younis, M. I. (2005). Dynamics of MEMS resonators under superharmonic and subharmonic excitations. *Journal of Micromechanics and Microengineering*, 15(10), 1840–1847. DOI 10.1088/0960-1317/15/10/008.
8. Amer, Y. A., El-Sayed, A. T., El-Bahrawy, F. T. (2015). Torsional vibration reduction for rolling mill's main drive system via negative velocity feedback under parametric excitation. *Journal of Mechanical Science and Technology*, 29(4), 1581–1589. DOI 10.1007/s12206-015-0330-8.
9. Amer, Y. A., El-Sayed, A. T., Kotb, A. A. (2016). Nonlinear vibration and of the Duffing oscillator to parametric excitation with time delay feedback. *Nonlinear Dynamics*, 85(4), 2497–2505. DOI 10.1007/s11071-016-2840-z.
10. Yaman, M. (2009). Direct and parametric excitation of a nonlinear cantilever beam of varying orientation with time-delay state feedback. *Journal of Sound and Vibration*, 324(3–5), 892–902. DOI 10.1016/j.jsv.2009.02.010.
11. Alhazza, K. A., Majeed, M. A. (2012). Free vibrations control of a cantilever beam using combined time delay feedback. *Journal of Vibration and Control*, 18(5), 609–621. DOI 10.1177/1077546311405700.
12. Cai, G. P., Yang, S. X. (2006). A discrete optimal control method for a flexible cantilever beam with time delay. *Journal of Vibration and Control*, 12(5), 509–526. DOI 10.1177/1077546306064268.
13. Mirafzal, S. H., Khorasani, A. M., Ghasemi, A. H. (2016). Optimizing time delay feedback for active vibration control of a cantilever beam using a genetic algorithm. *Journal of Vibration and Control*, 22(19), 4047–4061. DOI 10.1177/1077546315569863.
14. Amer, Y. A., El-Sayed, A. T., Abd El-Salam, M. N. (2020). Position and velocity time delay for suppression vibrations of a hybrid Rayleigh-Van der Pol-Duffing oscillator. *Sound & Vibration*, 54(3), 149–161. DOI 10.32604/sv.2020.08469.

15. Abdelhafez, H., Nassar, M. (2016). Effects of time delay on an active vibration control of a forced and self-excited nonlinear beam. *Nonlinear Dynamics*, 86(1), 137–151. DOI 10.1007/s11071-016-2877-z.
16. Liu, C. X., Yan, Y., Wang, W. Q. (2019). Primary and secondary resonance analyses of a cantilever beam carrying an intermediate lumped mass with time-delay feedback. *Nonlinear Dynamics*, 97(2), 1175–1195. DOI 10.1007/s11071-019-05039-w.
17. El-Ganaini, W. A., Saeed, N. A., Eissa, M. (2013). Positive position feedback (PPF) controller for suppression of nonlinear system vibration. *Nonlinear Dynamics*, 72(3), 517–537. DOI 10.1007/s11071-012-0731-5.
18. El-Sayed, A. T., Bauomy, H. S. (2016). Nonlinear analysis of vertical conveyor with positive position feedback (PPF) controllers. *Nonlinear Dynamics*, 83(1–2), 919–939. DOI 10.1007/s11071-015-2377-6.
19. Ferrari, G., Amabili, M. (2015). Active vibration control of a sandwich plate by non-collocated positive position feedback. *Journal of Sound and Vibration*, 342, 44–56. DOI 10.1016/j.jsv.2014.12.019.
20. Niu, W., Li, B., Xin, T., Wang, W. (2018). Vibration active control of structure with parameter perturbation using fractional order positive position feedback controller. *Journal of Sound and Vibration*, 430, 101–114. DOI 10.1016/j.jsv.2018.05.038.
21. Omid, E., Mahmoodi, S. N. (2015). Sensitivity analysis of the nonlinear integral positive position feedback and integral resonant controllers on vibration suppression of nonlinear oscillatory systems. *Communications in Nonlinear Science and Numerical Simulation*, 22(1–3), 149–166. DOI 10.1016/j.cnsns.2014.10.011.
22. EL-Sayed, A. T., Bauomy, H. S. (2018). Outcome of special vibration controller techniques linked to a cracked beam. *Applied Mathematical Modelling*, 63, 266–287. DOI 10.1016/j.apm.2018.06.045.
23. Jun, L. (2010). Positive position feedback control for high-amplitude vibration of a flexible beam to a principal resonance excitation. *Shock and Vibration*, 17(2), 187–203. DOI 10.1155/2010/286736.
24. Omid, E., Mahmoodi, S. N. (2015). Multimode modified positive position feedback to control a collocated structure. *Journal of Dynamic Systems, Measurement, and Control*, 137(5), 1–7. DOI 10.1115/1.4029030.
25. Nayfeh, A. H., Mook, D. T. (1979). *Nonlinear oscillations*. New York: Wiley.
26. Marinc, V., Herisanu, N. (2012). *Nonlinear dynamical systems in engineering: Some approximate approaches*. USA: Springer Science & Business Media.

Appendix

$$H_1(T_1) = \frac{i\hat{\beta}_1\omega_1^3A^3 + 5i\hat{\beta}_2\omega_1^5A^4\bar{A} - \hat{\gamma}_1A^3 - 5\hat{\gamma}_2A^4\bar{A} + 2\hat{\delta}_1\omega_1^2A^3 + 6\hat{\delta}_2\omega_1^2A^4\bar{A}}{-8\omega_1^2},$$

$$H_2(T_1) = \frac{-i\hat{\beta}_2\omega_1^5A^5 - \hat{\gamma}_2A^5 + 2\hat{\delta}_2\omega_1^2A^5}{-24\omega_1^2}, H_3(T_1) = \frac{\hat{\lambda}_1B}{\omega_1^2 - \omega_2^2}, H_4(T_1) = \frac{\hat{f}}{2(\omega_1^2 - \Omega^2)} \text{ and}$$

$$H_5(T_1) = \frac{\hat{\lambda}_2A}{\omega_2^2 - \omega_1^2}, r_{11} = -\left[\frac{\alpha_1}{2} + \frac{9\beta_1\omega_1^2}{8}a_{10}^2 + \frac{25\beta_2\omega_1^4}{16}a_{10}^4\right], r_{12} = \left[\frac{f}{2\omega_1} \cos(\phi_{10})\right],$$

$$r_{13} = \left[\frac{\lambda_1}{2\omega_1} \sin(\phi_{20})\right], r_{14} = \left[\frac{\lambda_1}{2\omega_1} a_{20} \cos(\phi_{20})\right],$$

$$r_{21} = \left[\frac{\sigma_1}{a_{10}} + \frac{3\delta_1\omega_1}{4}a_{10} - \frac{9\gamma_1}{8\omega_1}a_{10} - \frac{25\gamma_2}{16\omega_1}a_{10}^3 + \frac{5\delta_2\omega_1}{4}a_{10}^3\right],$$

$$r_{22} = -\left[\frac{f}{2\omega_1 a_{10}} \sin(\phi_{10})\right], r_{23} = \left[\frac{\lambda_1}{2\omega_1 a_{10}} \cos(\phi_{20})\right], r_{24} = -\left[\frac{\lambda_1}{2\omega_1 a_{10}} a_{20} \sin(\phi_{20})\right],$$

$$r_{31} = -\left[\frac{\lambda_2}{2\omega_2} \sin(\phi_{20})\right]$$

$$r_{32} = 0, r_{33} = -\left[\frac{\alpha_2}{2}\right], r_{34} = -\left[\frac{\lambda_2}{2\omega_2} a_{10} \cos(\phi_{20})\right],$$

$$r_{41} = \left[\frac{\sigma_1}{a_{10}} + \frac{3\delta_1\omega_1}{4}a_{10} - \frac{9\gamma_1}{8\omega_1}a_{10} - \frac{25\gamma_2}{16\omega_1}a_{10}^3 + \frac{5\delta_2\omega_1}{4}a_{10}^3 - \frac{\lambda_2}{2\omega_2a_{20}}\cos(\phi_{20}) \right],$$

$$r_{42} = -\left[\frac{f}{2\omega_1a_{10}}\sin(\phi_{10}) \right], r_{43} = \left[\frac{\sigma_2 - \sigma_1}{a_{20}} + \frac{\lambda_1}{2\omega_1a_{10}}\cos(\phi_{20}) \right],$$

$$r_{44} = \left[\left(\frac{\lambda_2a_{10}}{2\omega_2a_{20}} - \frac{\lambda_1a_{20}}{2\omega_1a_{10}} \right) \sin(\phi_{20}) \right],$$

$$\Gamma_1 = -(r_{11} + r_{22} + r_{33} + r_{44}),$$

$$\Gamma_2 = r_{22}(r_{11} + r_{33} + r_{44}) + r_{44}(r_{11} + r_{33}) + r_{11}r_{33} - r_{12}r_{21} - r_{13}r_{31} - r_{14}r_{41} - r_{24}r_{42} - r_{34}r_{43},$$

$$\begin{aligned} \Gamma_3 = & r_{11}(r_{24}r_{42} + r_{34}r_{43} - r_{22}(r_{33} + r_{44}) - r_{33}r_{44}) + r_{22}(r_{13}r_{31} + r_{14}r_{41} - r_{33}r_{44} + r_{34}r_{43}) \\ & + r_{33}(r_{12}r_{21} + r_{14}r_{41} + r_{24}r_{42}) + r_{44}(r_{12}r_{21} + r_{13}r_{31}) + r_{12}(r_{23}r_{31} + r_{24}r_{41}) \\ & + r_{14}(r_{21}r_{42} + r_{31}r_{43}) + r_{34}(r_{13}r_{41} + r_{23}r_{42}) \end{aligned}$$

$$\begin{aligned} \Gamma_4 = & r_{11}(r_{22}(r_{33}r_{44} - r_{34}r_{43}) - r_{42}(r_{24}r_{33} + r_{23}r_{34})) - r_{22}(r_{41}(r_{14}r_{33} + r_{13}r_{34}) + r_{31}(r_{13}r_{44} + r_{14}r_{43})) \\ & - r_{33}(r_{12}(r_{21}r_{44} + r_{24}r_{41}) + r_{14}r_{21}r_{42}) - r_{12}(r_{31}(r_{23}r_{44} + r_{24}r_{43}) - r_{34}(r_{21}r_{43} - r_{23}r_{41})) \\ & + r_{42}(r_{31}(r_{13}r_{24} - r_{14}r_{23}) - r_{13}r_{21}r_{34}). \end{aligned}$$